Tracking of a Moving Target by Improved Potential Field Controller in Cluttered Environments

Marwa Taher[1], Hosam Eldin Ibrahim[2], Shahira Mahmoud[3], Elsayed Mostafa[4]

[1] Automatic Control Department, Tibben Institute for Metallurgical studies
Cairo, 11913, Egypt

[2] Faculty of Engineering, Helwan University
Cairo, 11792, Egypt

[3] Faculty of Engineering, Helwan University
Cairo, 11792, Egypt

[4] Faculty of Engineering, Helwan University
Cairo, 11792, Egypt

Abstract

In this paper, robot tracking of a moving target in cluttered environments by using an improved potential field controller is proposed. Genetic algorithms are used to improve the potential field controller by optimizing the forces applied to the robot. This improvement makes the robot path much more smoother during the tracking. A measure of smoothness is used to guide the genetic algorithm during the optimization. Of course more smoothing gives less distance and more speed to reach the goal. The optimized controller is simulated with different cases on Windows Vista using Matlab Software. These cases include environments with single obstacle up to three obstacles and multi-knee corridor. Results are compared to previous work, illustrating the superiority of the proposed work. Tracking of a moving target in the same cases are also simulated.

Keywords: *Obstacle avoidance, Relative distance, Virtual sensor, Genetic Algorithm, Artificial potential field.*

1. Introduction

Through the advance in mobile robots from path guidance methods to autonomous mobility, resulting on obstacle avoidance of robots have emerged steadily over the years including directional command methods, such as artificial potential fields [1-5], and speed-space commands, such as the curvature foundation system [6-9]. However, most previous results remain a challenging problem as most existing methods have not considered the mobility of robots and obstacles. If a robot moves very slowly, most of the established algorithms can be applied to avoid obstacles. These algorithms cause a robot to move very slowly for obstacle avoidance. As it moves faster and faster, avoidance control is more difficult and the robot tends to collide more frequently with obstacles. The virtual sensor concept was introduced in [10] is used in our work. This concept is similar to that of the Doppler Effect. When a robot heads to an obstacle, the distance on the robot sensor is longer than the virtual sensor. Likewise, the physical distance on the robot sensor is shorter than the virtual one when it goes away from an obstacle.

The philosophy of the artificial potential field approach which is used in the current work can be schematically described as: the robot moves in a field of forces. The position to be reached is an attractive pole for the robot and obstacles are repulsive surfaces for the manipulator parts. The net force determines the behaviour of the robot against the objects in its environment.

In this paper, optimization of the potential field controller forces applied on the robot making the robot path much smoother, shorter and with high speed will be demonstrated. Efficiency of robot obstacle avoidance will be regarded too. The Genetic Algorithm (GA) is used to select the optimum factors of the repulsive and the attractive forces in the offline state which can be then applied on the robot in the online state. The optimum factors are those who make the robot motion more smoother. Simulation on Matlab is executed for testing the performance of the improved potential field controller in the task of robot obstacle avoidance. The simulation results are then used to compare the performance of the proposed system and the established system in [10] to evaluate the proposed system effectiveness. Tracking a moving target in cluttered environments by using the improved potential field controller is also simulated on Matlab.

This paper is organized as follows. In Section 2, Avoidability Measure and Odometry will be discussed briefly. Section 3 illustrates the Artificial Potential Field theory. Section 4 explains the determination of the

optimum factors of the potential field controller forces using GA and illustrates the GA fitness function which is used in our work. Section 5 shows the performance of the proposed system by simulation in four different cases. In addition, comparison with the established system in [10] will be reviewed. Conclusion and future work are given in Section 6.

2. Avoidability Measure and Odometry

The efficiency of robot's motion is determined by the smoothness, the speed, and selection of the shortest path to reach to the goal with obstacle avoidance. The proposed system is concerned with satisfying high efficiency of the robot's motion. The speed and direction of robot motion play a key role for efficient and safe control. The mobility is taken into account through the use of a virtual sensor as in [10]. Relative mobility of the robot is detected by computing its odometry. The avoidability measure depends on the virtual sensors and the robot mobility.

2.1 Avoidability Measure (AVM)

The distance between robot and obstacle can be used for collision detection. If the robot moves, the probability of collision depends on the speed of the robot. Therefore, the AVM of a moving robot can be defined by the distance between the robot and the obstacle, and the speed of the robot. All of computations of avoidability measure using virtual sensor in [10] are used in the proposed system.

2.2 Odometry

The proposed system depends on the angle approach [11, 12] to compute the odometry. Fig. 1 [13] gives a very rough overview about the geometrical relationship of this approach.

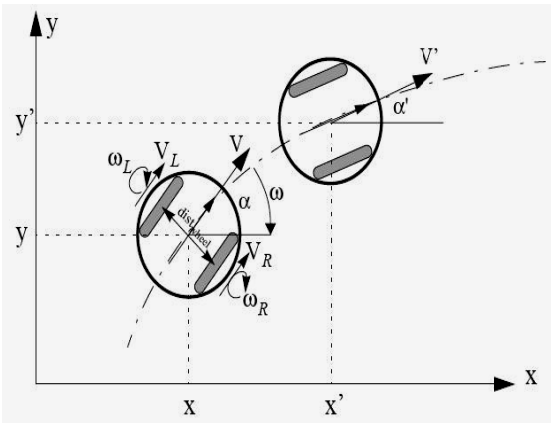

Fig. 1 Overview about the geometrical relationship.

The rotation speed ω is proportional to the speed difference of the two wheels as follows:

$$\omega = \frac{V_L - V_R}{dist_{wheel}} = \frac{r_{wheel} \cdot (\omega_L - \omega_R)}{dist_{wheel}} \quad (1)$$

Where : VL and VR are the forward speeds for the left and the right wheels respectively, distwheel is the distance between the two wheels, rwheel is the radius of the wheel, ωLand ωR are the rotational speeds for the left and the right wheels respectively.

The forward speed V is proportional to the average wheel speed as follows:

$$V = \frac{V_L + V_R}{2} = \frac{r_{wheel}}{2} \cdot (\omega_L + \omega_R) \quad (2)$$

$$\left.\begin{matrix} x' = x + V\cos\alpha \cdot \Delta t \\ y' = y + V\,sin\alpha \cdot \Delta t \\ \alpha' = \alpha + \omega\Delta t \end{matrix}\right\} \quad \left.\begin{matrix} \Delta x = V\,cos\alpha \cdot \Delta t \\ \Delta y = V\,sin\alpha \cdot \Delta t \\ \Delta\alpha = \omega\Delta t \end{matrix}\right\} \quad \begin{bmatrix} \dot{x} \\ \dot{y} \\ \dot{\alpha} \end{bmatrix}$$

$$= \begin{bmatrix} V\,cos\alpha \\ V\,sin\alpha \\ \omega \end{bmatrix} \quad (3)$$

Where: x, y are the coordinates of the robot in the x-y plane, α is the heading angle of the robot, Δt is the time step, x', y' are the new location of the robot after time step in the x-y plane, α' is the new heading angle of the robot.

3. Artificial Potential Field

An artificial potential field $U_{art}(t)$ consists of the attractive force U_g (t) and the repulsive force $U_k(t)$. The distance between the nth actual sensor on the robot and the obstacle d_{ro} (t, n) in [1] is replaced with the distance between the nth virtual sensor on the robot and the obstacle $v_{svr}(t, n)$ in [10].

$$U_{art}\big(P_r(t), P_0(t), P_g\big) = U_k\big(P_r(t), P_0(t)\big) + U_g\big(P_r(t), P_g\big) \quad (4)$$

Where: $P_r(t)$ is the robot position at time t, $P_o(t)$ is the obstacle position at time t, and P_g is the goal position.

$$U_k\big(P_r(t), P_0(t)\big) = \begin{cases} \frac{1}{2}K_r\left(\frac{1}{vsv_r(t)} - \frac{1}{\varepsilon}\right) & if\ vsv_r(t) \le \varepsilon \\ 0 & if\ vsv_r(t) > \varepsilon \end{cases}$$

$$\text{where} \quad \varepsilon = 1 \quad (5)$$

$$U_g\big(P_r(t), P_g\big) = \frac{1}{2}K_a|P_r(t) - P_g|^2 \quad (6)$$

Where: K_r is the repulsive force factor, ε is the distance between the robot and the obstacle in which the repulsive force must be applied on the robot, K_a is the attractive force factor.

The force on robot pose $P_r(t)$ can be calculated from the gradient function of the artificial potential field as:

$$F_{art} = -grad\left(U_{art}\left(P, P_0(t), P_g\right)\right)|P = P_r(t)$$
$$= -grad\left(U_{art}\left(P, P_0(t)\right)\right) - grad\left(U_{art}\left(P, P_g\right)\right)$$
$$= F_O\left(P_r(t)\right) + F_g\left(P_r(t)\right) \quad (7)$$

As the robot approaches the obstacle the repulsive force $F_o(P_r(t))$ increases. On the other hand, the attractive force to the goal $F_g(P_r(t))$ will be decreased as it approaches its goal. Therefore, the net force from the artificial potential fields enables the robot to smoothly move to the goal.

4. Determining the Optimum Factors and Fitness function

The attractive and repulsive coefficients K_a, K_r of the forces are determined empirically in [10], that shouldn't grantee a fast and smooth robot path. To overcome that empirical factors determination, one of the optimization techniques such as (GA) can be used to better determine those factors.

The fitness function which is used in GA optimizer is the smoothness (SM) that is defined as a criterion of the evaluation to measure the various robot trajectories.

$$SM = \sum_{n=0}^{m}(\varphi_n - \varphi_{n-1}) \quad (8)$$

$$\varphi_n = tan^{-1}\frac{y_n - y_{n-1}}{x_n - x_{n-1}} \quad (9)$$

Where : m = the last pose number of robot trajectory, x_n and y_n represent the robot position at n[th] sampling time. φ_n is the angle between current and former position at n[th] sampling time.

First the optimum parameters for the potential field controller are obtained in offline state. It includes guided random search operation using GA to determine the optimum factors for K_r and K_a which are the factors of the repulsive and the attractive forces respectively. Four different environments for testing the improved potential field controller are used. These cases are those typically used in [10]. The best fitness and the best individual figures are yielded after applying the GA optimizer for these four cases. The following subsections illustrate these four cases.

4.1 One Obstacle in the Workspace

In Case 1, there is only one obstacle and one robot in the workspace. The start point is (0,0) and the end point is (4,2). After applying the GA optimizer, the optimum values of K_a, K_r according to our fitness function are 13.4210, 0.2628. The best fitness and the best individual figures for this case are shown in Fig. 2.

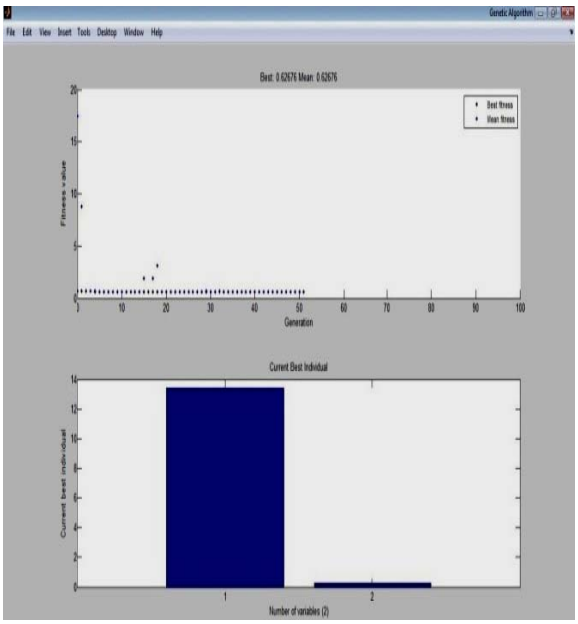

Fig. 2 The best fitness and the best individual figures which are yielded after applying the GA for case 1.

4.2 Two Obstacles in the Workspace

In Case 2, there are 1 robot and 2 obstacles in the workspace. The start point is (0,0) and the end point is (4,3) in this case. The GA optimizer gives the optimum values of K_a, K_r which are 15.7406, 0.1927. The best fitness and the best individual figures are shown in Fig. 3.

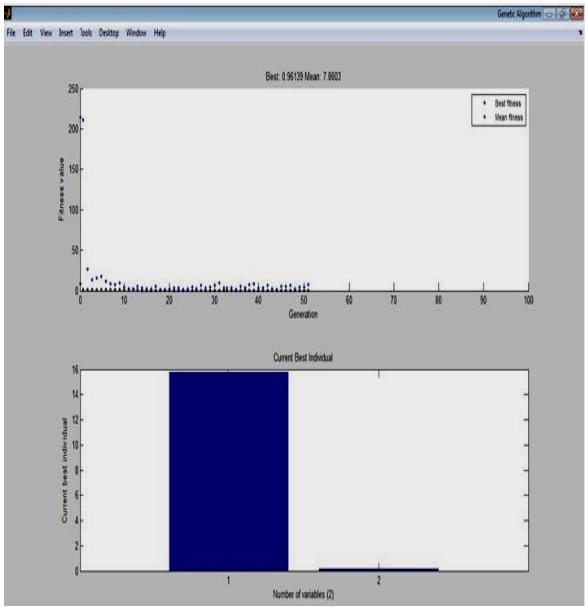

Fig. 3 The best fitness and the best individual figures which are yielded after applying the GA for case 2.

4.3 Three Obstacles in the Workspace

In Case 3, 1 robot and 3 obstacles are in the workspace. The start and the end points are equivalent to Case 2. The GA optimizer gives the optimum values of K_a, K_r which are 20.7208, 0.0285 while the best fitness and the best individual figures are shown in Fig. 4.

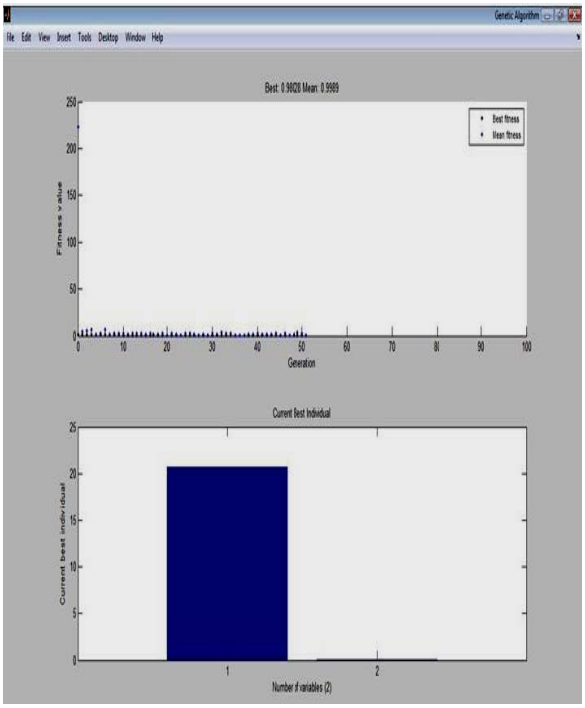

Fig. 4 The best fitness and the best individual figures which are yielded after applying the GA for case 3.

4.4 Corridor Environment

In Case 4, the robot moves in the corridor and two obstacles are given. The start and the end points are (2,0) and (6.5,6.5), respectively. The GA optimizer gives the optimum values of K_a, K_r which are 13.7519, 0.7037. Due to the complex path in the fourth case, the best fitness and the mean fitness have big values, relative to the previous cases, during all generations as shown in Fig. 5. Although this case is complex but the result is optimized by using GA optimizer. The best fitness and the best individual figures are shown in Fig. 5.

Now, the optimum values of K_a and K_r which are obtained from the offline state in each case will be applied at the online state. The following section shows the robot's motion at the online state in the four cases after applying the optimum values of K_a and K_r.

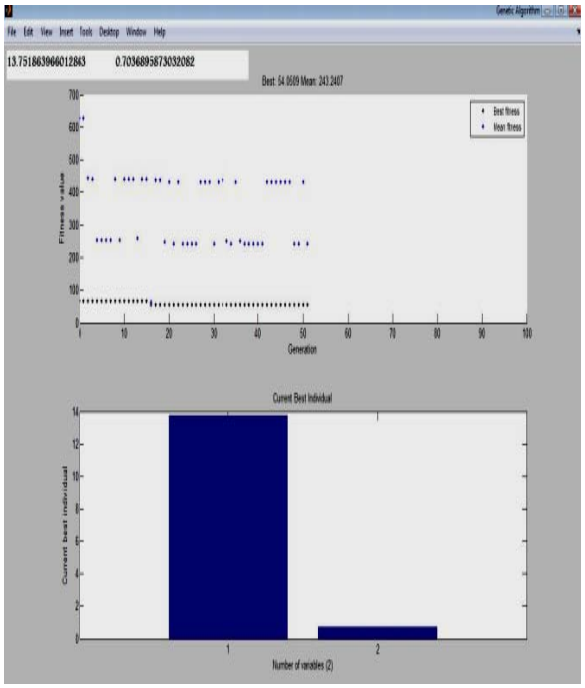

Fig. 5 The best fitness and the best individual figures which are yielded after applying the GA for case 4.

5. Simulation Results

This section shows the simulation results of robot motion in four different environments at three states. The first state is the robot motion to go to a static goal at each environment using its K_a and K_r values. The second state is the robot motion to go to a static goal at each environment using the average values of K_a and K_r of the four environments. The third state is robot tracking of a moving target using the average values of K_a and K_r of the four environments. Sections 5.1, 5.2 and 5.3 show the simulation results in the four environments at these three states respectively.

5.1 Robot Motion to reach a Static Goal in each environment with its K_a and K_r values

To show the optimization achieved in the performance of the proposed method, it is compared with [10].

5.1.1 One Obstacle in the Workspace

The motion paths in case 1 are shown in Fig. 6(a, b). The start point and the end point are as mentioned in section 4.1. The robot with empirical values of K_a and K_r displays slower evasive action, as in Fig. 6(a), than the proposed system using the optimum values of K_a and K_r as in Fig. 6(b). Fig. 6(a) shows abrupt changes in the robot's path. However, the second robot displays smoother changes.

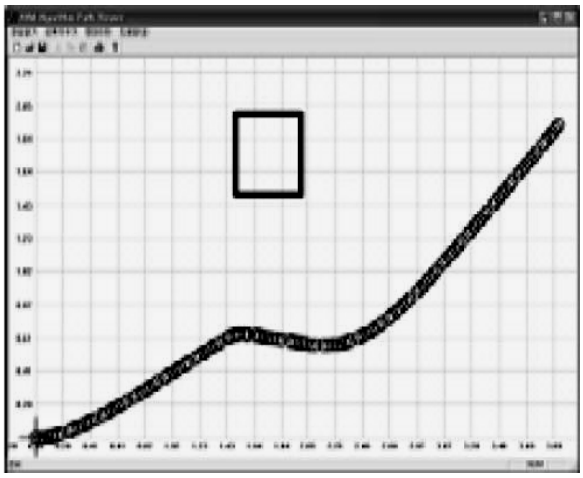

(a)

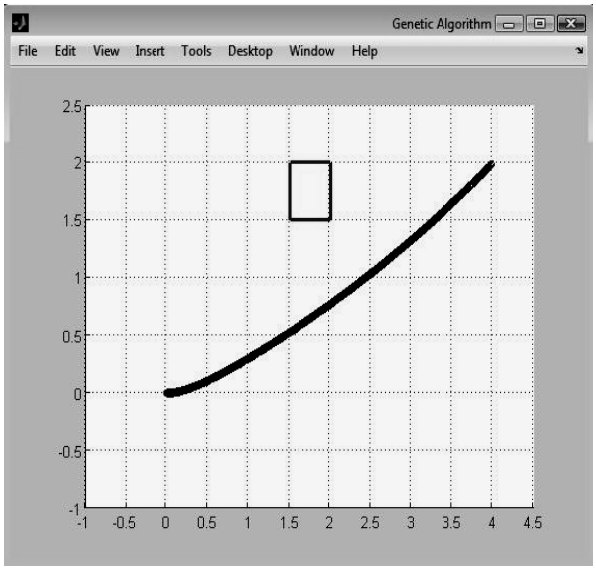

(b)

Fig. 6 Robot trajectories in Case 1. (a) Without Optimization [10], (b) With Optimization.

5.1.2 Two Obstacles in the Workspace

Case 2 displays abrupt directional changes on the robot's path which uses empirical values of K_a and K_r as shown in Fig. 7(a). These abrupt changes are occurred due to a slower response of a repulsive force to the obstacle and an attractive force to the goal. On the contrary, the robot's path using the proposed method is rounder and smoother as shown in Fig. 7(b). The start point and the end point are as mentioned in section 4.2.

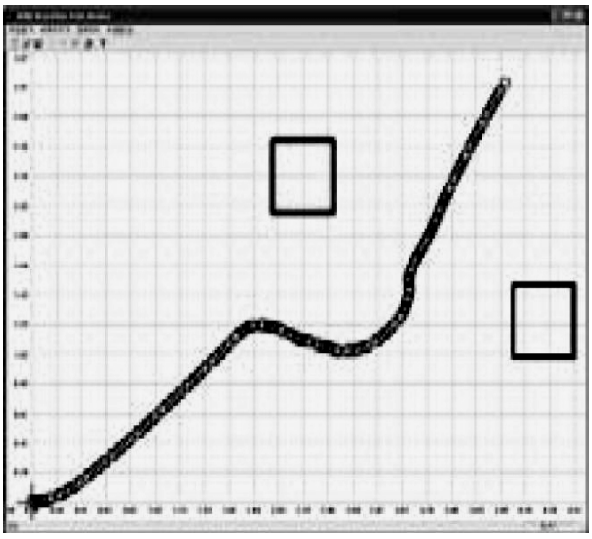

(a)

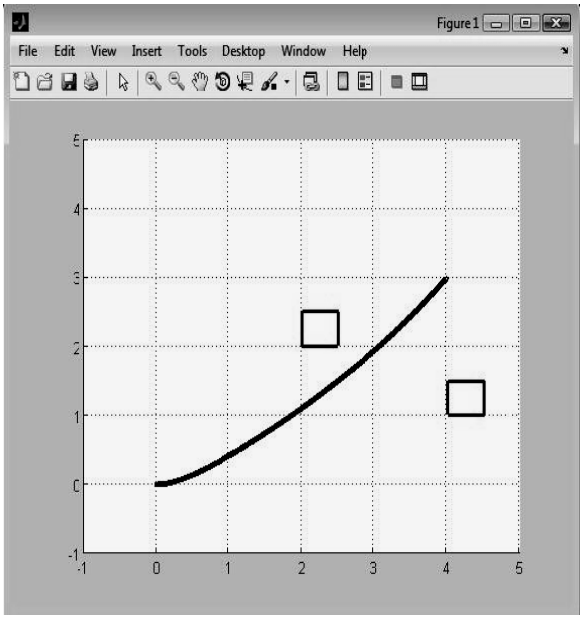

(b)

Fig. 7 Robot trajectories in Case 2. (a) Without Optimization [10], (b) With Optimization.

5.1.3 Three Obstacles in the Workspace

Fig. 8 shows the robot trajectory for Case 3. The start point and the end point are as mentioned in section 4.2.The robot in previous work makes zigzagging in its path due to slow evasive action.

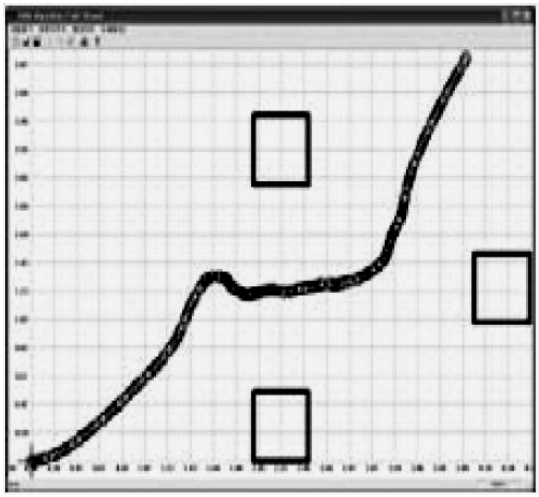

(a)

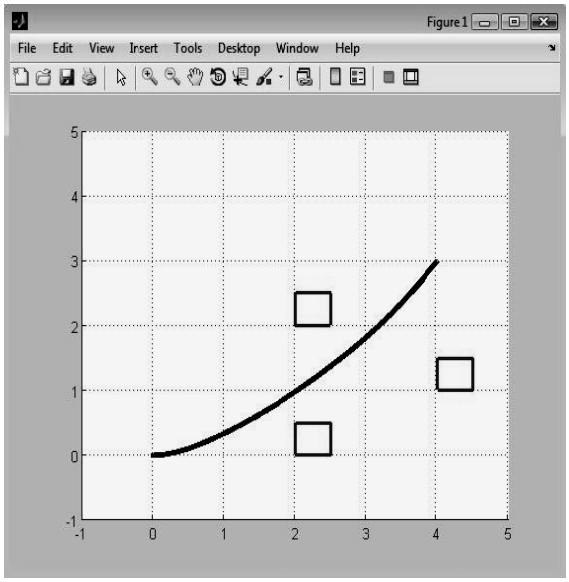

(b)

Fig. 8 Robot trajectories in Case 3. (a) Without Optimization [10], (b) With Optimization.

5.1.4 Corridor Environment

In Case 4, the robot moves in the corridor and two obstacles are given. Fig.9 shows the robot trajectory. The start point and the end point are as mentioned in section 4.4.

The simulation results show that using the proposed method the robot has better performances with respect to smoothness in all cases. The smoothness is computed using the fitness function for each case and compared with the smoothness recorded by the previous work in Table 1. It shows the large optimization is occurred in the proposed system.

As shown from the Table 1 a large optimization of the smoothness is occurred. When the path of the robot is smoother it means that the robot takes shortest path and it takes less time to go to the goal.

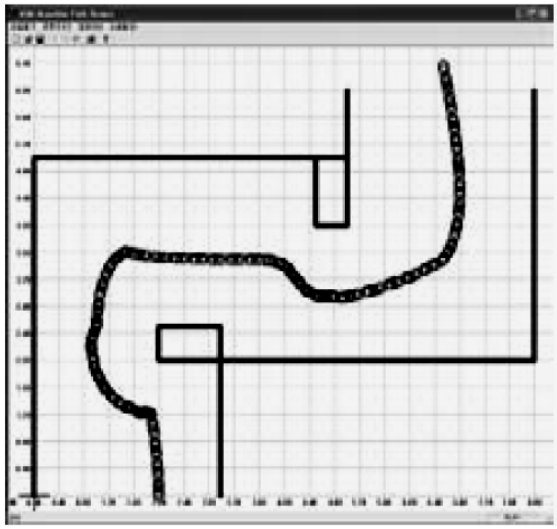

(a)

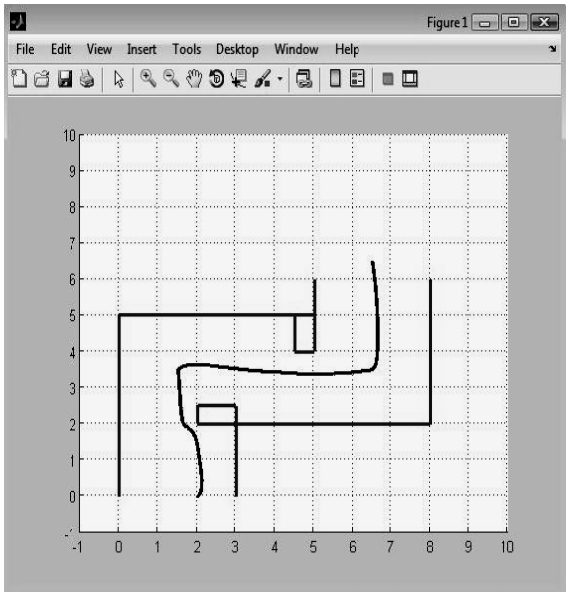

(b)

Fig. 9 Robot trajectories in Case 4. (a) Without Optimization [10], (b) With Optimization.

5.2 Robot Motion to reach a Static Goal in each environment using the average values of K_a and K_r

The average of the values of K_a and K_r in the four cases are computed which are 15.9086 and 0.296, respectively. These two average values are applied onto the four cases. The paths of the robot at these four cases with these average values are shown in Fig. 10. The smoothness achieved at each case using the average values of K_a and K_r is shown also in Table 1.

Table 1: The Comparison of Smoothness between the Proposed Method Using GA and the Previous Work

Smoothness	***Case 1***	***Case 2***	***Case 3***	***Case 4***
Without GA	133.7309	303.4949	510.1164	1420.295
With GA	0.6268	0.9614	0.9803	54.0509
Using Average Factors	0.6593	21. 8747	42.061	55. 5763

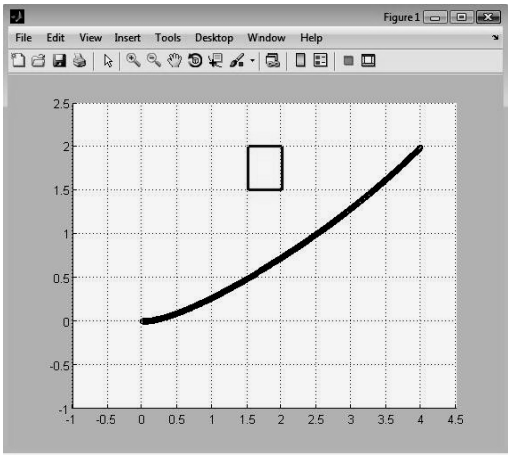

(a)

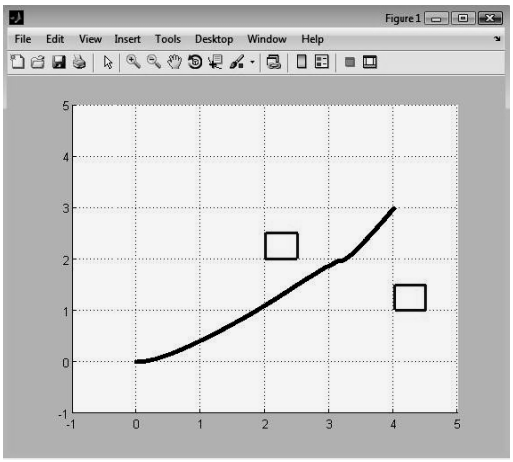

(b)

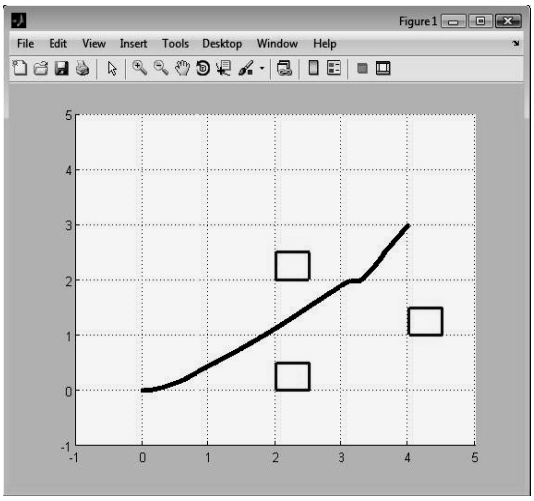

(c)

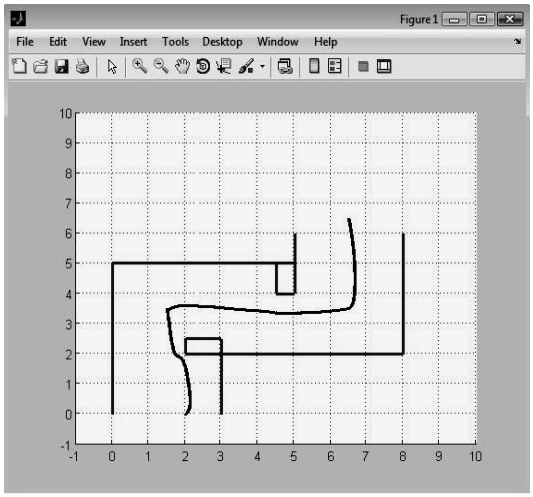

(d)

Fig. 10 Robot trajectories with the average values (a) Case 1, (b) Case 2, (c) case 3, (d) Case 4.

5.3 Tracking of a Moving Target

In this simulation, we have two robots which are called Robo1 and Robo2. Robo1 should track Robo2 and Robo2 should go to its static goal (end-point). Tracking and motion of the two robots at the four environments are shown in this section.

Using the average values of K_a and K_r of the four cases, and computing the forces which are applied on the two robots make each of them move to its goal smoothly as shown in the Fig.11 (a, b, c, and d). Where, the red path represents Robo1's tracking path which follows Robo2, and the blue path represents Robo2's path to reach to the end point which is coloured by a green colour. The start position of Robo1 and Robo2, and the end point location at each case are shown in Table 2.

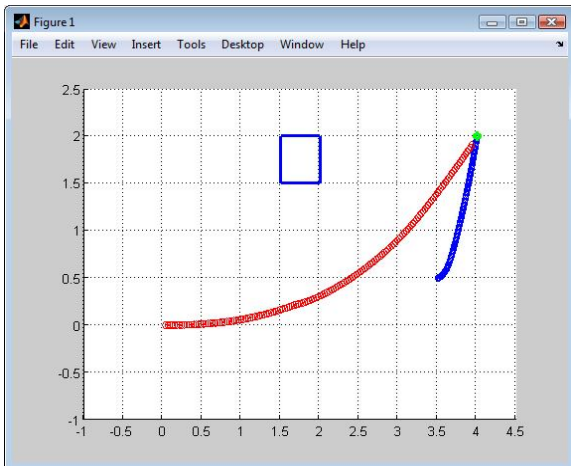

(a)

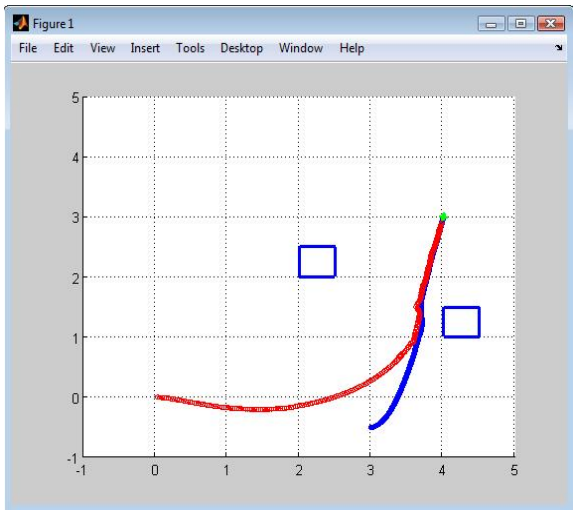

(b)

(c)

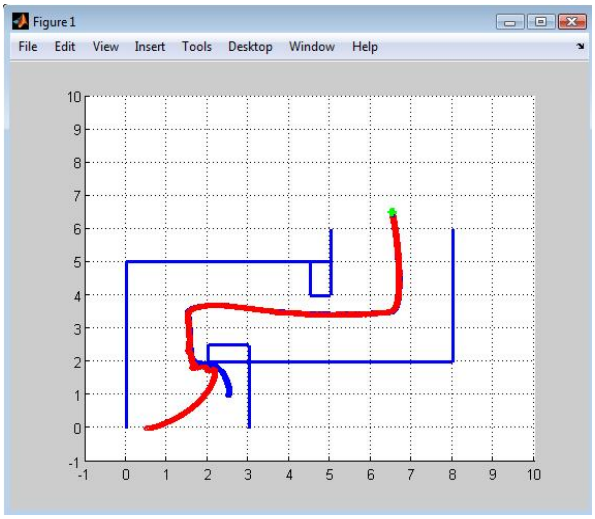

(d)

Fig. 11 Robo1 tracks robo2 in (a)case 1, (b) case 2, (c) case 3, (d) case 4.

Table 2: The Comparison of Smoothness between the Proposed Method Using GA and the Previous Work

Position	***Case 1***	***Case 2***	***Case 3***	***Case 4***
Robo1	(0, 0)	(0, 0)	(0, 0)	(0.5, 0)
Robo2	(3.5, 0.5)	(3, -0.5)	(3, 1)	(2.5, 1)
End-Point	(4, 2)	(4, 3)	(5, 2)	(6.5, 6.5)

6. Conclusions

In this paper, computation of odometry is used to reflect the mobility of moving robot. GA optimizer is used in different robot environments to select the optimum factors of the forces to reach the goal while avoiding obstacles. The optimized parameters are tested in four different environments. The results show the superiority of the optimized controller generally and inclusively compared to the work in [10]. The average of the computed factors by GA optimizer for the four cases is applied again onto the same cases, while the smoothness in our work remains better than the results in [10]. Graceful optimization regarding the path motion is achieved. Another application for the improved potential field controller is introduced, in which a moving goal is tracked by a robot. The moving goal is controlled by the improved potential field controller. The potential fields controlling the tracking robot are: attractive one (from the moving goal), and repulsive one from the obstacles. Again we use the improved potential field controller with its average values of Ka and Kr for applying the forces on the tracking robot. Tracking a moving target is also simulated in the same four given environments. Simulation results shows how the tracking robot succeeds in tracking the moving goal

smoothly. The real implementation of the proposed work can be done as a future work.

References

[1] O. Khatib, "Real-Time Obstacle Avoidance for Manipulators and Mobile Robots", Int. J. Robotics Research, Vol. 5, No. 1, Spring 1986, pp. 90-98.

[2] J. Borenstein and Y. Koren, "The Vector Field Histogram-Fast Obstacle Avoidance for Mobile Robots", IEEE Trans. on Robotics Automation, Vol. 7, No. 3, June 1991, pp. 278-288.

[3] J. Borenstein and Y. Koren, "Obstacle Avoidance with Ultrasonic Sensors", IEEE Journal of Robotics, Vol. 4, No. 2, 1988, pp. 213-218.

[4] E. Shi, T. Cai, C. He and J. Guo, "Study of the New Method for Improving Artificial Potential Field in Mobile Robot Obstacle Avoidance", Proc. of IEEE International Conference on Automation and Logistics, 2007, pp 282-286.

[5] J. Gong, Y. Duan, Y. Man, and G. Xiong, "VPH+: An Enhanced Vector Polar Histogram Method for Mobile Robot Obstacle Avoidance", Proc. of International Conference on Mechatronics and Automation, 2007, pp. 2784-2788.

[6] R. G. Simmons, "The Curvature-Velocity Method for Local Obstacle Avoidance", Proc. of IEEE International Conference on Robotics and Automation, April 1996, pp.3375-3382.

[7] N. Y. Ko, R. G. Simmons, and K. S. Kim, "A Lane Based Obstacle Avoidance Method for Mobile Robot Navigation", Journal of Mechanical Science and Technology, Vol. 17, No. 11, 2003, pp. 1693-1703.

[8] A. Kelly, "An Intelligent Predictive Control Approach to the High Speed Cross Country Autonomous Navigation Problem", Tech Report CMU-CS-TR-95-33, School of Computer Science, Carnegie Mellon University, 1995.

[9] C. Schlegel, "Fast Local Obstacle Avoidance under Kinematic and Dynamic Constrains for a Mobile Robot", Proc. of IEEE/RSJ International Conference on Intelligent Robots and Systems, 1998, Vol. 1, pp. 594- 599.

[10] Dong Jin Seo, Nak Yong Ko, and Jung Eun Son, "A Method for Combining Odometry and Distance Sensor Information for Effective Obstacle Avoidance of Autonomous Mobile Robots", International Journal of Control, Automation, and Systems, Vol. 8, No. 3, 2010, pp. 597-603.

[11] Guy Campion et al., Structural Properties and Classification of Kinematic and Dynamic Models of Wheeled Mobile Robots, IEEE Transactions on Robotics and Automation, Vol. 12, No. 1, pp. 47-62, February 1996.

[12] C. Canudas de Wit and O. J. Sørdalen, "Exponential Stabilization of Mobile Robots with Nonholonomic Constraints", IEEE Transactions on Automatic Control, Vol. 37, No. 11, pp.1792 – 1797, November 1992.

[13] Philip Machler, "Robot Positioning by Supervised and Unsupervised Odometry Correction", PhD thesis, Department of Information, École Poly Technique Federal of Lausanne, 1998.

Marwa Taher received her B.Sc. degree in Computer Engineering t, and her M.Sc. degree in Electronic Engineering from Helwan University, Cairo, Egypt in 2001 and 2006, respectively. She has two published papers at M.Sc. degree. She is currently a Research Assistant at Tibben Institute for Metallurgical Studies, Cairo, Egypt. Her research interests include robot motion, tracking and their industrial applications.

Hossam Eldin Ibrahim received his B.Sc. degree in Communications & Electronics Engineering, his M.Sc. degree in Computer Engineering, and his Ph.D. degree in Computer Engineering from Helwan University, Cairo, Egypt, in 2000, 2004, and 2009 respectively. He has three published papers at M.Sc. degree, and seven published papers at Ph.D. degree. He is currently a Teacher at Electronics, Communication & Computer Department, Faculty of Engineering, Helwan University.

Shahira Mahmoud received her B.Sc. degree in Communications & Electronics Engineering, her M.Sc. degree in Communications & Electronics Engineering, and her Ph.D. degree in Communications & Electronics Engineering from Helwan University, Cairo, Egypt, in 1997, 2000, and 2006 respectively. She has seven published papers. She is currently a Teacher at Electronics, Communication & Computer Department, Faculty of Engineering, Helwan University.

Elsayed Mostafa Saad is a Professor of Electronic Circuits, Faculty of Engineering,Univ. of Helwan.He received his B.Sc. degree in Electrical Engineering(Communication section) from Cairo Univ. ,his Dipl.-Ing. degree and Dr.-Ing degree from Stuttgart Univ. , West Germany ,at 1967,1977 and 1981 respectively . He became an Associate Prof. and a Professor in 1985 , and 1990 respectively. He was an International scientific member of the ECCTD, 1983. He is Author and/or Co-author of 132 scientific papers. He is a member of the national Radio Science Comittee,member of the scientific consultant committee in the Egyptian Eng. Syndicate for Electrical Engineers, till lMay 1995 , Member of the Egyptian Eng. Sydicate,Member of the European Circuit Society(ECS), Member of the Society of Electrial Engineering(SEE).